World Academy of Science, Engineering and Technology
International Journal of Electronics and Communication Engineering
Vol:12, No:9, 2018

# Fully Printed Strain Gauges: A Comparison of Aerosoljet-Printing and Micropipette-Dispensing

Benjamin Panreck, Manfred Hild



***Abstract*—**Strain sensors based on a change in resistance are well established for the measurement of forces, stresses, or material fatigue. Within the scope of this paper, fully additive manufactured strain sensors were produced using an ink of silver nanoparticles. Their behavior was evaluated by periodic tensile tests. Printed strain sensors exhibit two advantages: Their measuring grid is adaptable to the use case and they do not need a carrier-foil, as the measuring structure can be printed directly onto a thin sprayed varnish layer on the aluminum specimen. In order to compare quality characteristics, the sensors have been manufactured using two different technologies, namely aerosoljet-printing and micropipette-dispensing. Both processes produce structures which exhibit continuous features (in contrast to what can be achieved with droplets during inkjet printing). Briefly summarized the results show that aerosoljet-printing is the preferable technology for specimen with non-planar surfaces whereas both technologies are suitable for flat specimen.

***Keywords*—**Aerosoljet-printing, micropipette-dispensing, printed electronics, printed sensors, strain gauge.

## I. Introduction

IN this paper the additive manufacturing of strain gauges using two different ways of printing electronics is shown. Strain sensors based on a change in resistance are well established for measuring forces, stresses, or material fatigue. The benefit of printed strain gauges is a decrease in production steps because it works without glueing a foil and it is more eco-friendly than the classical subtractive technology. Additionally, the extreme flexibility to adapt to the shape and size to the specimen respectively to the direction of the forces makes it more versatile. Some use cases are shown in [3], [6], [7].

Depending on the printing technology, non-flat specimen in more than one dimension are, in contrast to classical foil strain gauges, no problem.

The silver nanoparticle ink PRELECT TPS 50 (Clariant) was the basic material used for the conductive part of the strain gauges. The used printing technologies are Aerosoljet-printing (AJP) with the AerosolJet 200 (Optomec Inc.) and micropipette-dispensing (MPD) with the Microplotter II (Sonoplot Inc.). While these technologies are very different at first glance, they have one thing in common.

Both technologies produce so called 'continuous-features' or 'vector-prints'. This means that the lines and arcs are printed as if they were painted with a pencil – with equal shape and line-width in all printing directions. Inkjet printing (IJP), the most widely used technology in the field of printed electronics, cannot produce continuous features because of the underlying technology which forms lines by overlapping spots. Particular attention must be paid to the different printing results in the printing direction and against the printing direction. For further information see Seifert et al. [8].

Manfred Hild is with the Neurorobotics Research Laboratory, Beuth University of Applied Sciences Berlin, Germany.

Benjamin Panreck is with the Neurorobotics Research Laboratory, Beuth University of Applied Sciences Berlin, Germany (e-mail: bpanreck@beuth-hochschule.de).

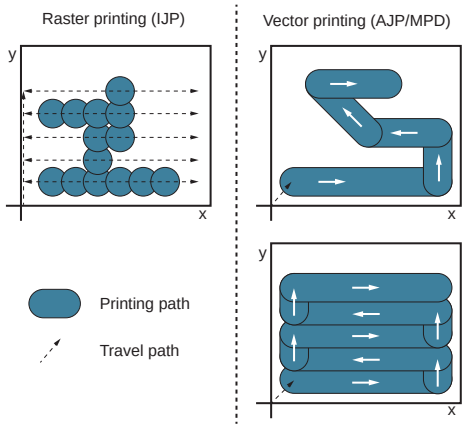


Fig. 1 Comparison of raster-based IJP in single-nozzle mode and vector-based AJP/MPD

Fig. 1 illustrates the difference between raster-prints (IJP) and vector-prints (AJP and MPD). It also shows how to print filled areas by using serpentine filling as an example. This is useful, e.g. for contact pads.

## II. Printed Strain Gauges

Commercial strain gauges are available in various sizes and shapes. The right choice is dependant on the use case, specifically the shape of the specimen and the magnitude and direction of the force to be measured. Frequently, disturbing variables have to be compensated for, e.g. the temperature expansion of the substrates. The ability to print these sensors substantially extends the range of possibilities. With these advances, it is possible to print strain sensors to areas which are too small or too difficult to access with foil-based sensors. It enables printing adapted shapes for every single piece.

For the following analysis, reduced shapes without temperature compensation and with pads for the measuring cables were printed. The outer dimension of the shapes is $5\,mm$ x $3\,mm$, the size of the pads $0.4\,mm$ x $0.4\,mm$. The meander-shaped measuring grid consists of ten loops. Fig. 2 shows the vector graphic designed in SonoDraw for MPD. The shape for the prints with AJP was designed in Autodesk AutoCAD and looks identical.

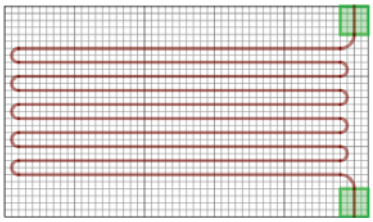

Fig. 2 Vector graphic of strain gauge sensor with outer dimensions of $5\,mm$ x $3\,mm$ and pads with size of $0.4\,mm$ x $0.4\,mm$

After printing, the ink was cured with a convection oven of type N 30/65HA (Nabertherm) for 3 hours at $250\,°C$.

## III. Substrate

The substrate used is an aluminum specimen with alloy AW2017A and a thickness of $2\,mm$. The shape is from type H in accordance with the national norm DIN 50125 [2], which recommends certain shapes for different types of specimen in tensile stress tests.

After CNC-milling and deburring the specimen was cleaned with a tenside-free jewelry cleaner in an ultrasonic bath and finally with isopropanol. An isolating layer of urethane was applied with the URETHAN 71 spray (CRC Kontakt Chemie). The isolation layer was cured at room temperature for two days. For further information about a printed isolating layer see [10].

### A. Aerosoljet-Printing

Aerosoljet-printing opens the possibility to print a wide range of materials. With the ultrasonic atomizer (UA), viscosities in range of $1\,cp$ to $10\,cp$ are possible. Using the pneumatic atomizer (PA) the range is extended to a viscosity up to $1,000\,cp$. For this paper we used the UA.

The used ink was a solution of PRELECT TPS 50 silver ink and distilled water in proportion of (3:1) by volume.

The principle of AJP is shown in Fig. 3. $0.8\,ml$ of the ink solution were used and filled in the atomizer glass vessel. The ultrasonic speaker, which produces the aerosol from the aqueous solution, is controlled between $100\,mA$ and $500\,mA$. The aerosol is then transported with a controlled flow of nitrogen (atomizer gas) to the deposition head. Due to the transport, the aerosol agglomerates to particles with a diameter of about $1\,\mu m$ to $5\,\mu m$. In the deposition head is a second nitrogen (sheath gas) source with a controlled flow to focus the aerosol when it exits the nozzle. The sheath gas additionally prevents the nozzle from clogging. AJP is a contactless manufacturing technology. Thus, the distance between the tip of the nozzle and the substrate can vary between $2\,mm$ and $5\,mm$.

Using this technology, the minimum line width of printed structures on substrate is currently about $10\,\mu m$, making it one of the additive printing technologies with the thinnest print results for electronic use. Characteristic for AJP are the so called ‘sprinkles’. These are loose particles of silver agglomerates around the printed structure. They are clearly visible later on in Fig. 9a as well.

Table I shows the printing parameters used for AJP.

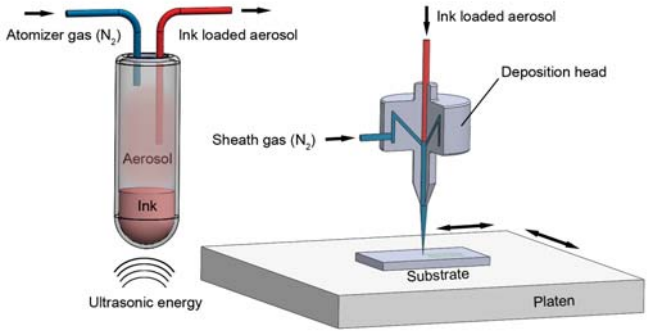


Fig. 3 Principle of AJP: A schematic of the aerosol jet process using an ultrasonic atomizer

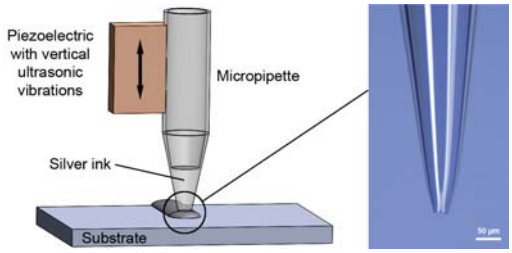


Fig. 4 Principle of MPD: Fluid deposition via ultrasonic pumping. This example shows a pipette with a tip diameter of $30\,\mu m$

### B. Micropipette-Dispensing

In contrast to AJP the MPD is not a contactless technology. The central element is a small vial made of glass, ending in a tiny tip with a diameter between $1\,\mu m$ and $60\,\mu m$. This pipette is glued on a vertical oscillating piezoelectric. The viscosity of the solution can range from $1\,cp$ to $450\,cp$. Fig. 4 shows the used type of pipette with a tip diameter of $30\,\mu m$. The exact diameter and the angle of the tip in reference to the longitudinal axis of the pipette differs with every exemplar because the reproducibility in production of this thin glas pipettes is very low. The angle is very important considering the ink deposition in every print direction and also for the risk of damaging the tip. This presents the user with further challenges during printing and makes the result less reproducible.

The function of the piezoelectric is to pump the ink in and out of the pipette. To load the ink, two distinct methods are possible. The first option is to make use of the capillary forces in the pipette by digging the tip into a reservoir of ink, with the capillary forces pulling the liquid upwards. The second is filling in the ink at the wide open end of the glass vial [5].

Because of the contacting principle special care needs to be taken not to damage the pipette by letting the tip touch the substrate in an uncontrolled way. For this task, a function exists that allows moving the pipette towards the substrate in steps of $5\,\mu m$. In case of contact, the resonance of the oscillating piezoelectric changes and the system stops the movement.

Fig. 5 shows a topography map which was measured by the Microplotter II with a $30\,\mu m$-pipette. The resolution of $5\,\mu m$ is limited in all three axes by the positioning system of the plotter. This map can be used to vertically offset the printed

TABLE I
PRINTING PARAMETERS OF AJP

| Parameter | Value |
|---|---|
| Atomizer gas | $22\,sccm$ |
| Sheath gas | $65\,sccm$ |
| Ultrasonic atomizer current | $500\,mA$ |
| Ink temperature | $30\,°C$ |
| Platen temperature | $RT\ (26\,°C)$ |
| Printing speed | $1\,\frac{mm}{s}$ |
| Nozzle diameter | $150\,\mu m$ |
| Bubbler | empty |
| Layer | 1 |

TABLE II
PRINTING PARAMETERS OF MPD

| Parameter | Value |
|---|---|
| Piezoelectric amplitude | $0.7\,V$ |
| Ink temperature | $RT\ (26\,°C)$ |
| Platen temperature | $RT\ (26\,°C)$ |
| Printing speed[1] | $1 \cdot 10^3$ |
| Printing acceleration[1] | $1 \cdot 10^5$ |
| Pipette diameter | $30\,\mu m$ |
| Topography map resolution in x | $300\,\mu m$ |
| Topography map resolution in y | $500\,\mu m$ |
| Layer | 2 |

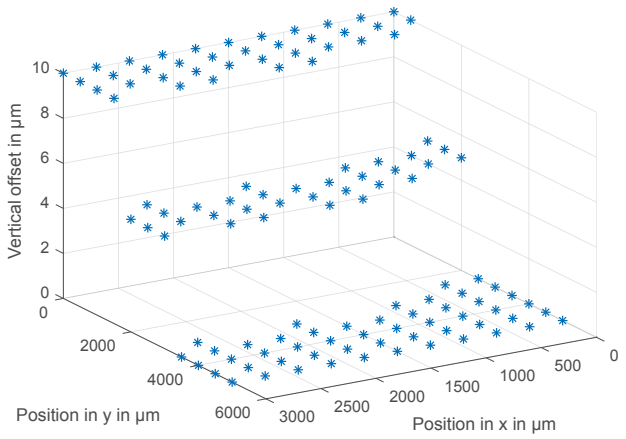


Fig. 5 Topography of substrate measured with pipette of the microplotter

shapes.

Depending on the solvents it could happen that they evaporate before or during printing, thus preventing a successful print. For this reason polyethylene glycol (PEG) 400 was added as an additional solvent to the silver ink PRELECT TPS 50 in proportion of (1:1) by volume which does not evaporate at room temperature. Another solution that tackles the challenge from a technological point of view is shown in [1].

Table II shows the printing parameters used for MPD.

[1]This value is unitless and refers to the setting of the Microplotter II.

### C. Differences of Printed Structures between AJP and MPD

For inspecting the printed structures the optical microscope Keyence VHX-500F was used. For SEM[2] images the Stereoscan 100 (Cambridge Instruments) was used. Due to the isolating surface of the urethane layer an about hundred nanometer thick layer of Au had to be sputtered on top with the Desk II (Denton Vacuum).

Fig. 6 shows a full overview of the printed strain gauges with AJP and MPD. On a coarse view they look very similar. With MPD, only the curves are looking slightly irregular. Fig. 7 illustrates the different line widths of the structures. The AJP lines are about $22\,\mu m$ and the MPD lines about $50\,\mu m$ wide. Conspicuous is the widely differing structure of the contact-pads. While the serpentine-structure achieved by AJP is clearly visible, the lines of ink from MPD have fused before curing.

The height maps in Fig. 8 are measured with the optical microscope and a good estimation of the altitude profiles. They show that the layer thickness of the printed lines with AJP is $\approx 2.4\,\mu m$ and with MPD is $\approx 3.7\,\mu m$.

The images in Fig. 9 are made with the SEM. They clearly show the bigger particles from AJP resulting from agglomeration and the existence of sprinkles around the printed structure. On the other hand, the lines are much thinner and without conspicuous irregularities.

In Fig. 9c a filled area achieved by AJP is shown. This is for easier contact to the measurement connection. The area is meander filled and the endpoints at which the table reverses the movement direction, are visible by the hillocks. Due to the decrease and increase in printing speed at the endpoints, additional deposition occurs. The effect can be reduced by converting the edges to arcs.

Fig. 9d shows the most important challenge faced by MPD. Most of the mackles resulted from a damaged glas pipette. The pipette was damaged during the printing process by a scratch in the substrate, which is visible in the center of the picture. The broken off parts were left in the print result.

## IV. TENSILE TESTS

For tensile tests the printed strain gauges have to be connected with a resistance measurement device. The used setup are enameled wires with skinned ends that were connected electrically with conductive silver (Leitsilber 200 by Demetron) which have a low resistance. The silver was cured by room temperature for 1 hour. To protect this connection mechanically, the conductive silver points and ends of wires were covered with conductive glue (Electric Paint by BARE Conductive) without touching the measurement grid.

The tensile testing machine was the inspekt retrofit QTS 50kN by Hegewald & Peschke Mess- und Prueftechnik GmbH. The measurement and documentation of ohmic resistance was realized with the source-measurement-unit (SMU) B2902A by Keysight Technologies.

For comparison the reference strain gauge FAE-25-35-S13EL-G (Micro Measurements/Vishay) with

[2]SEM: scanning electron microscope

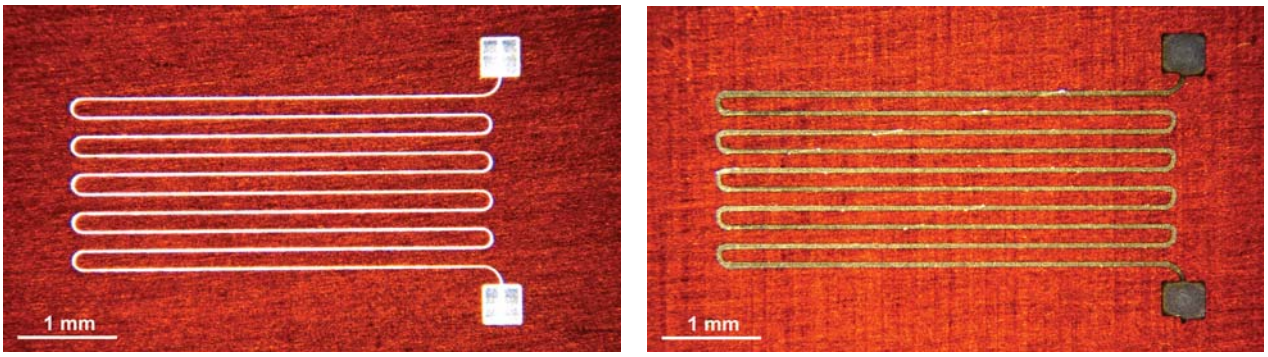


(a) AJP (b) MPD

Fig. 6 Microscope pictures of the full printed strain gauges with AJP and MPD

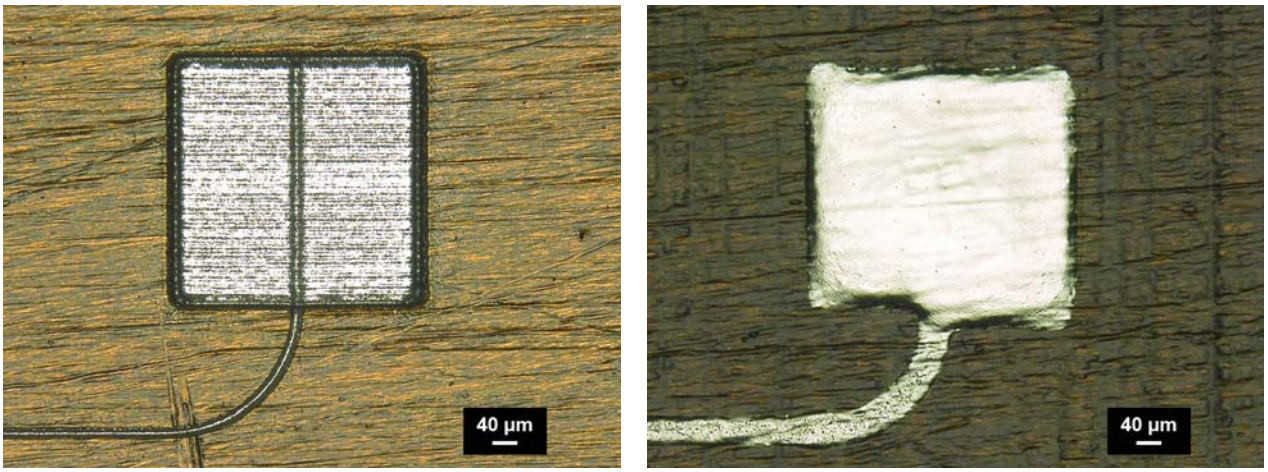


(a) AJP (b) MPD

Fig. 7 Microscope pictures of printed pads with AJP and MPD

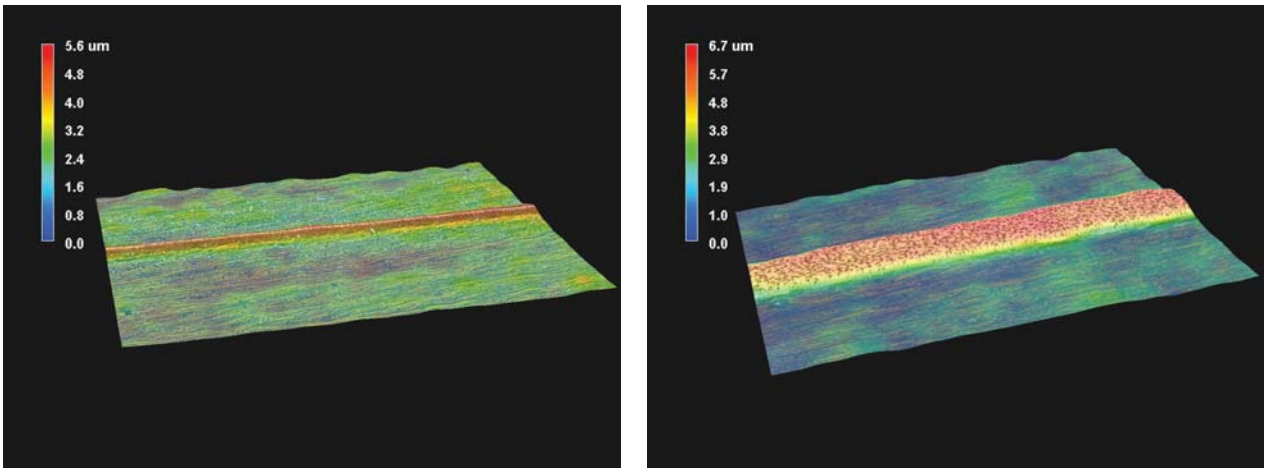


(a) AJP (b) MPD

Fig. 8 Height measurement with microscope of printed lines with AJP and MPD

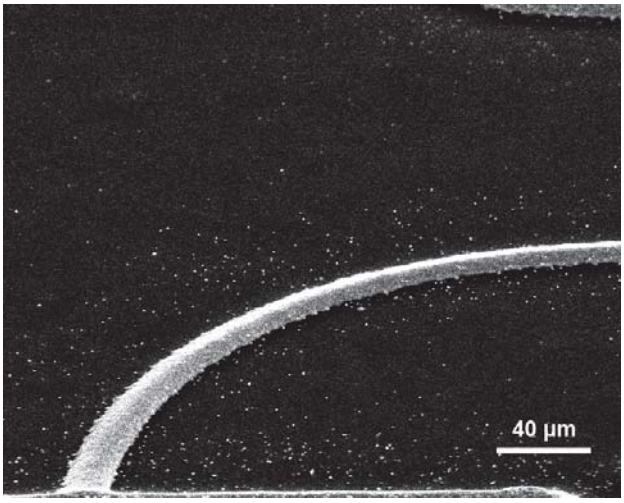


(a) Printed line with AJP. Agglomeration of ink and sprinkles are clearly visible

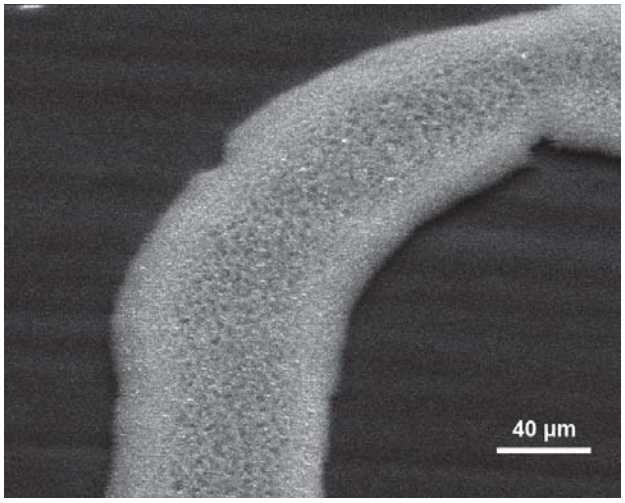


(b) Printed line with MPD. Much finer particles than with AJP, no sprinkles but irregular structure width

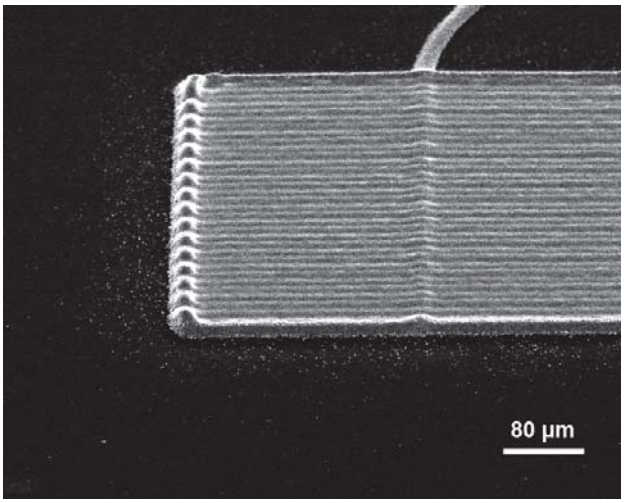


(c) Meander filled pad, printed with AJP. The endpoints at which the table reverses the movement direction, are visible by the hillocks

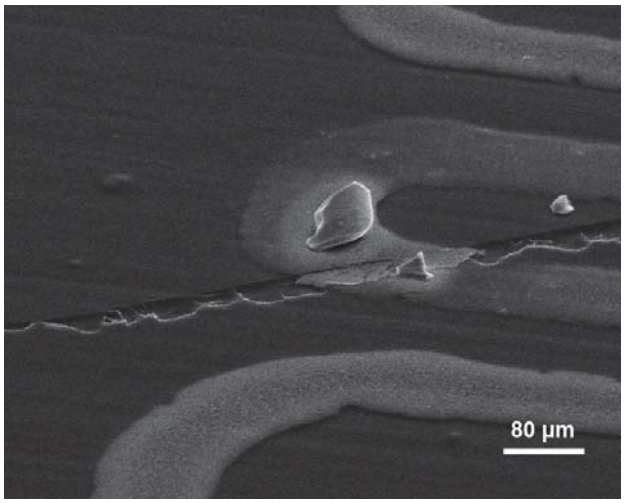


(d) Printed line with MPD. In the center of the picture a part of the micropipette is visible. Due to the scratch in the substrate, it was damaged while printing and remained in the print result

Fig. 9 SEM-pictures of printed strain gauges with AJP and MPD

(a) Tensile test with reference strain gauge

(b) Clamped tensile specimen with AJP strain gauges

Fig. 10 Structure of the tensile test

nominal grid resistance of $350\,\Omega$ was chosen. It was applied directly to the aluminum specimen, in compliance with the manufacturer's instructions.

Seven strain gauges were printed and prepared for measurement for each of the two examined printing technologies, totalling 14 strain gauges.

Fig. 10 shows the test setup. The test procedure was force controlled. Before each test procedure started, an initial tension of $200\,N$ was added. From here, the load was cycled from $200\,N$ to $700\,N$ for 100 cycles with each cycle lasting $10\,s$.

Fig. 11 displays an excerpt of the tensile test results with the reference strain gauge and one representative strain gauge from AJP and MPD each. This seems reasonable, as the results within the groups of AJP sensors and MPD sensors were in a similar range. The first (top) graph shows the applied force F to the specimen and the resulting difference in length $\Delta l$. The time axis correlates with the steps of the three graphs beneath. The red curve depicts the floating average of the resistance and the green line is the arithmetic average of the whole resistance

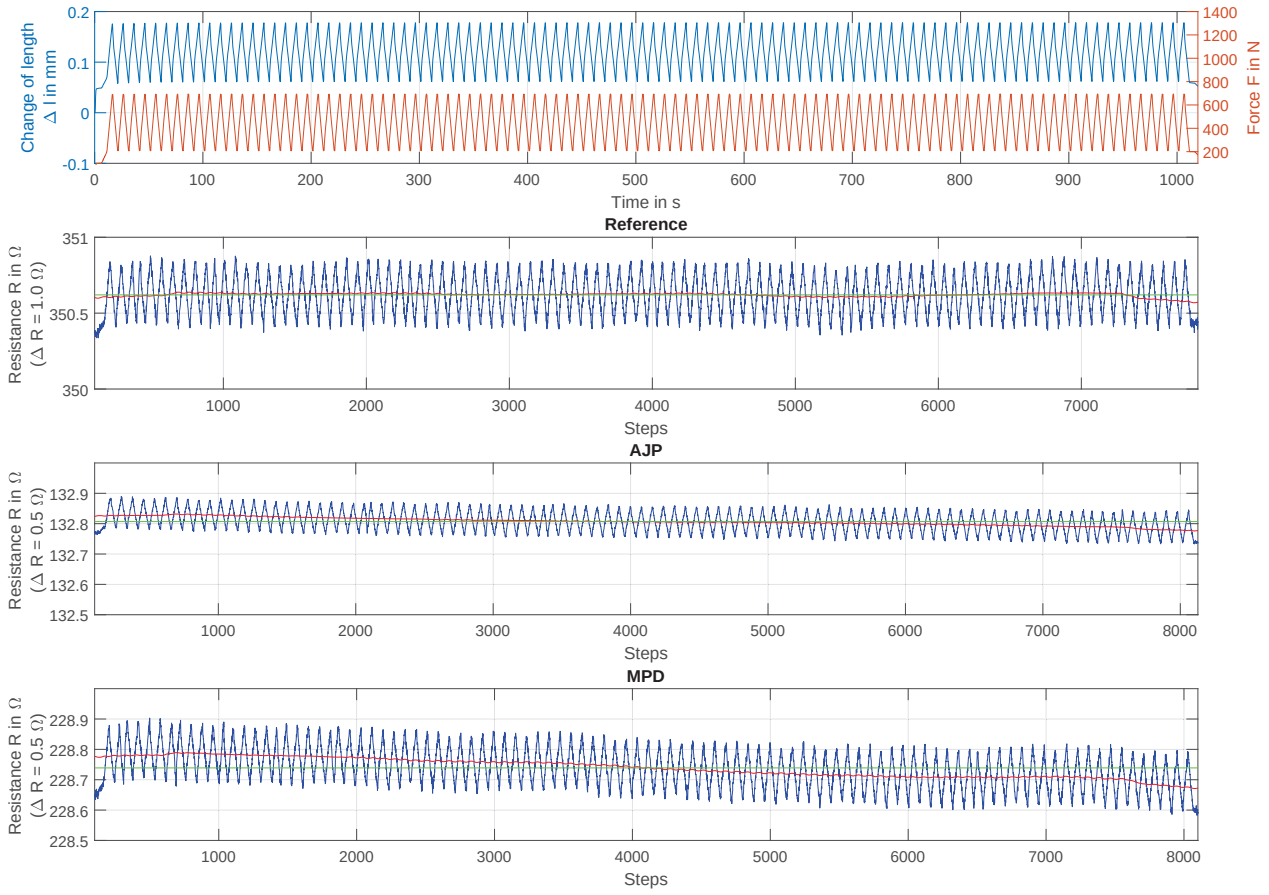


Fig. 11 Results of tensile tests with reference strain gauge and one representative strain gauge from AJP and MPD each. Red: Floating average of the resistance, Green: Arithmetic average of the entire resistance measurement

measurement. The difference between the green line an the red curve is a quantity for the drift of the sensor resistance. While the resistance of the reference sensor is nearly constant there is a conspicuous drift in the resistance of the printed sensors. Over the 17 minutes of testing per strain gauge the resistance drifts in mean with $\Delta R_{Drift,AJP} \approx -45\,m\Omega$ and $\Delta R_{Drift,MDP} \approx -70\,m\Omega$.

## V. Conclusion

In this paper the printing technologies aerosoljet-printing and micropipette-dispensing were compared based on the example of printed strain gauges.

In general it is possible to use either technology for the given task. In practice, MPD proved to be more troublesome due to the high likelihood of pipettes being damaged and even breaking on contact with the substrate. It is by far the most sensitive component in this system. We could identify three distinct damaging cases: Overly high piezoelectric voltage while trying to clean the tip after clogging because of a evaporated solvent, scratches or other irregularities in the substrate or lastly by measuring the topography map. The standard resolution of the $z$-axis with $5\,\mu m$ appears to not be high enough for some tasks. Considering the sensitivity of the system, we conclude that MPD is useful exclusively for flat specimen with a low degree of roughness.

Despite its drawbacks, MPD has a much lower acquisition and operation cost compared to AJP. While AJP needs nitrogen and variable tempered water for a stable process as well as to be cleaned rigorously from the atomizer to the nozzle after printing or after an ink change, MPD's maintenance consists of cleaning or replacing the pipettes and the microplates for the ink.

For small amounts of ink the AJP process is automatically ruled out, since a minimum amount of ink (in range of a few hundred microliters) is necessary for a stable aerosol while the MPD process works with amounts of a few picoliter as well.

The printing duration depends essentially on the printing speed. After tuning parameters accordingly, the difference is generally negligible.

The line width of the printed structures in AJP depends on every named parameter but is to be well tuned for the ink used [9]. In the case of MPD, further optimization is possible by increasing printing speed, decreasing nozzle diameter and choosing a more suitable ink respectively solvent.

Each of the 14 printed strain gauges is able to detect the applied tensile forces. The slightly negative drift in resistance over time and also the differing gradient between AJP and MPD require a further analysis like the one in [4].

## ACKNOWLEDGMENT

We thank Dr. Wilhelm H. Bruenger for his support with the SEM recordings.

The project was supported by European Regional Development Fund (EFRE), Project-no.: 2016011246


## REFERENCES

[1] A. M. Allanurov and A. Ye. Zdrok and A. G. Loschilov and N. D. Malyutin *Problem of ink evaporation while using plotter systems to manufacture printed electronic products*, Procedia Technology, Vol. 18, Pages 19–24, Elsevier, 2014.

[2] Norm DIN 50125 *Testing of metallic materials - Tensile test pieces*, December 2016, Deutsches Institut fuer Normung e.V., Beuth Verlag.

[3] F. L. Hammond and M. J. Smith and R. J. Wood *Estimating surgical needle deflection with printed strain gauges*, Engineering in Medicine and Biology Society (EMBC), 2014 36th Annual International Conference of the IEEE, Vol. 54, No. 2, Pages 6931–6936, IEEE, 2014.

[4] O. Kravchuk and M. Reichenberger *Properties and long-term behavior of nanoparticle based inkjet printed strain gauges*, Journal of Materials Science: Materials in Electronics, Vol. 27, No. 10, Pages 10934–10940, Springer, 2016.

[5] B. J. Larson and S. D. Gillmor and M. G. Lagally *Controlled deposition of picoliter amounts of fluid using an ultrasonically driven micropipette*, Review of Scientific Instruments, Vol. 75, No. 4, Pages 832–836, AIP, 2004.

[6] M. Maiwald and C. Werner and V. Zoellmer and M. Busse *INKtelligent printed strain gauges*, Sensors and Actuators A: Physical, Vol. 162, No. 2, Pages 198–201, Elsevier, 2010.

[7] B. Polzinger and J. Keck and V. Matic and W. Eberhardt *Inkjet and Aerosol Jet Printed Sensors on 2D and 3D Substrates*, Proceedings of the AMA Conferences, 2015.

[8] T. Seifert and E. Sowade and F. Roscher and M. Wiemer and Th. Gessner and R. R. Baumann *Additive manufacturing technologies compared: morphology of deposits of silver ink using inkjet and aerosol jet printing*, Industrial & Engineering Chemistry Research, Vol. 54, No. 2, Pages 769–779, ACS Publications, 2015.

[9] M. Smith and Y. S. Choi and C. Boughey and S. Kar-Narayan *Controlling and assessing the quality of aerosol jet printed features for large area and flexible electronics*, Flexible and Printed Electronics, Vol. 2, No. 1, IOP Publishing, 2017.

[10] V. Zoellmer, and E. Pál and M. Maiwald and Ch. Werner and D. Godlinski and D. Lehmhus and I. Wirth and M. Busse *Functional materials for printed sensor structures*, Proceedings of the 1st Joint International Symposium on System-Integrated Intelligence, No. 1, 2012.